Agricultural Water Management 239 (2020) 106233

Contents lists available at ScienceDirect

Agricultural Water Management

journal homepage: www.elsevier.com/locate/agwat

Winter wheat production on the Guanzhong Plain of Northwest China under projected future climate with SimCLIM

Zhen Zheng[a,d,e], Gerrit Hoogenboom[b,c], Huanjie Cai[d,e,*], Zikai Wang[f]

[a] Research Center of Fluid Machinery Engineering and Technology, Jiangsu University, 212013, China
[b] AgWeatherNet, Washington State University, Prosser, WA 99350-8694, USA
[c] Institute for Sustainable Food Systems, University of Florida, Gainesville, FL 32611, USA
[d] Key Laboratory for Agricultural Soil and Water Engineering in Arid Area of Ministry of Education, Northwest A&F University, Yangling, Shaanxi, 712100, China
[e] Institute of Water Saving Agriculture in Arid Areas of China, Northwest A&F University, Yangling, Shaanxi, 712100, China
[f] Zhenjiang Engineering Survey & Design Institute Co.Ltd, Zhenjiang, Jiangsu, 212013, China

ARTICLE INFO

Keywords:
Winter wheat
Climate change
Yield
CSM-CERES-wheat model

ABSTRACT

The Guanzhong Plain in China is particularly sensitive to climate change owing to its fragile ecological environment and geographic features. As a result, climate change is affecting the production of winter wheat in this area. In this study, we used SimCLIM (climate model) with the CSM-CERES-Wheat model to determine the impact of the climate change on the projected agricultural production of winter wheat in the Guanzhong Plain for 2020, 2040, 2060, 2080 and 2100 projections. Scenarios for three global climate models (GCMs) (BCC-CSM-1, CSIRO-MK3 − 6-0 and GFDL-CM3) and one greenhouse gas concentration pathway (RCP 4.5) were chosen. The results showed a warming trend in the Guanzhong Plain for both maximum and minimum temperature for the different GCMs. Although rainfall varied, the projected rainfall showed an increasing trend for February, June and December, and a decreasing trend for April, September and October. The solar radiation for the Baoji and Weinan area showed an upward trend, while the solar radiation in Wugong was greatly reduced. The maturity date of winter wheat for the three locations was reduced by 2.3–14.9 days compared with the reference year for different climate change scenarios. Water requirements of the winter wheat for the three locations under different GCMs were all increased compared with the reference year. Overall, winter wheat yield in Wugong and Weinan increased for the different GCMs scenarios during the 21st century.

1. Introduction

Future climate change is projected to be one of the major challenges for regional agricultural production worldwide. The global average temperature has increased about 0.74 °C for the past century and it is expected to increase further about 2.0 °C–5.4 °C by 2100 (IPCC, 2007; Tao et al., 2008). Generally, the increase in both maximum and minimum temperature might increase the water requirement for both rainfed and irrigated crops and could also increase the risk of heat stress during flowering for crops grown during the winter and spring, such as wheat and barley (Sommer et al., 2013).

Wheat (*Triticum aestivum* L.) is the most widely grown crop and cultivated on 220 million ha of farmland across the word (http://www.fao.org). About 21 % of the world's food depends on the wheat crop. However, global wheat production is facing challenges from global warming, water shortages, and other factors (Tao and Zhang, 2013). In addition, as a crop that prefers a relatively cool temperature, wheat growth and yield could be affected by climate change in many regions of the world. Wheat production is projected to decrease due to climate warming and changes in precipitation (Asseng et al., 2015, 2011). The growing evidence from various regions in the world has shown marked phenological changes in response to rising temperatures resulting in accelerated developmental rate and a shortened spring wheat growing season (Mo et al., 2016). Moreover, since both climate change and an increase in atmospheric CO_2 concentration vary, impacts of these factors on wheat growth and yields are complex and diverse (Karimi et al., 2018). Therefore, the vulnerability of wheat production in the future has become of key concern, as some regions could experience an increase in yield while other regions could experience a decrease in yield (Kristensten et al., 2011; Olesen et al., 2011).

The effects of climatic change on crop growth and productivity have been studied using data based on long-term historical field experiments (Peng et al., 2004; Tao et al., 2006). Additionally, in order to assess the effects of climate change on crop phenology, water demand, and

* Corresponding author at: No. 23 Weihui Road, Yangling, Shaanxi Province, 712100, China.
E-mail address: caihj@nwsuaf.edu.cn (H. Cai).

https://doi.org/10.1016/j.agwat.2020.106233
Received 9 September 2019; Received in revised form 23 April 2020; Accepted 24 April 2020

production and to provide adaptation strategies, climate models have been coupled with crop models (Yan et al., 2018; Yang and Mao, 2018). Process-based models make it possible to predict crop growth and yields under various weather conditions and crop management scenarios by simulating the comprehensive interactions of genetics * environment * management at a field scale (Cammarano et al., 2019; Chen et al., 2019; Gu et al., 2017; Liang et al., 2018; Liu et al., 2017a, b; Darko et al., 2016). The Cropping System Model (CSM)-CERES-Wheat, which is one of the main crop simulation models of the Decision Support System for Agrotechnology Transfer (DSSAT; Hoogenboom et al., 2019) has been used in several climate change studies (Amin et al., 2018; Bao et al., 2015a, b).

The Loess Plateau of China has a typical semi-arid to sub-humid monsoon climate and is influenced by the summer and winter monsoons annually. Limited precipitation with uneven spatial and temporal distribution, make the area vulnerable to climate change (Ding et al., 2018; Wang et al., 2012). The Guanzhong Plain, in the southern part of the Loess Plateua, is one of the three largest plains in the Loess Plateau. It is extremely sensitive to environmental challenges, such as climate variability and climate change (Zheng et al., 2016a). Air temperature in this area has increased by 0.38 °C decade^{-1} from 1961 to 2010 (Ding et al., 2016), which is about three times the global average of 0.13 °C decade^{-1} (Flato et al., 2013). Although there are variations across findings, different global climate models (GCMs) show that the region has the potential for a higher increase in temperature and a greater change in precipitation distribution (Liu et al., 2017a, b; He et al., 2015).

For this study, the DSSAT-CSM-CERES-Wheat model and three GCMs and one representative concentration pathways (RCP) scenarios 4.5 were used to simulate the potential long-term effects of future climate change on winter wheat phenology, water demand and grain yields for different projections. The specific objectives of this study were (1) to predict climate change based on different GCMs from 2020–2100, (2) to determine the potential impact of climate change for the projected years on rainfed winter wheat phenology and grain yield for three locations in the Guanzhong Plain, and (3) to determine the relationship between climate variables and winter wheat yield.

2. Method and materials

2.1. Study area

Winter wheat is one of the major food crops in China, accounting for 90 % of total wheat production. The Guanzhong Plain, located in Shaanxi province is one of the most ancient agricultural regions in China. The double-cropping rotation of summer maize and winter wheat is the dominant cropping system in the region. The study area is located in a continental monsoon climate zone with uneven rainfall distribution. Three different precipitation regions from west to east in the Guanzhong Plain were selected as the study sites for this study (Fig.1), Baoji (34.38 °N, 107.15 °E), Wugong (34.38 °N, 107.15 °E) and Weinan (34.38 °N, 107.15 °E). The long-term mean annual rainfall ranges from 330 to 620 mm and the reference evapotranspiration ranges from 400 to 550 mm, respectively, and more than 60 % of rainfall is concentrated between July to September. The altitude of the area ranges between 300 and 620 m above sea level.

2.2. Climate model

SimCLIM (http://www.climsystems.com/simclim) is an integrated model that can be customized by users to examine the effects and adaptations to climate variability and change, including extreme climate events. SimCLIM supports both spatial and site time-series analyses (Warrick, 2009). SimCLIM 2013 (Yin et al., 2013) relies mainly on the IPCC CMIP5 datasets. The baseline period generally ranges from 1986 to 2005 (centered on 1995), although it can also use 1961–1990 as the baseline period. In this study, we used 1961-1990 as the baseline period. Most of the basic spatial dataset (baseline and future) in SimCLIM 2013 is run at the global scale of 0.5°*0.5° resolution. The climate projections for different spatial scales can be generated from 1991 to 2100. The effects of greenhouse gas concentration (not emissions) trajectories are analyzed using four RCPs: RCP 2.6, RCP 4.5, RCP 6.0 and RC P8.5 as adopted by the IPCC for its Fifth Assessment Report (AR5) (IPCC, 2014). The four RCPs are named after a possible range of radiative forcing values in the year 2100 of 2.6, 4.5, 6.0 and 8.5 w/m^2, respectively. SimCLIM 2013 can display climate change information either for a single GCM or an ensemble of multiple GCMs. SimCLIM offers an easy and intuitive way to interpret the impacts of changes to daily climate data on agriculture, water supply, food risk, human health, energy demand, sea-level and ecosystem resilience (Abuodha, 2009; Storey, 2009; Warrick, 2007).

2.3. Winter wheat yield prediction

The CSM-CERES-Wheat model simulates the growth and development, productivity, water and nitrogen balances for wheat (Jones et al., 2003) based on crop genetics, including cultivar-specific parameters or cultivar coefficients. It is one of the most widely used crop models included in the DSSAT (Hoogenboom et al., 2011, 2019; Jones et al., 2003). The CSM-CERES-Wheat model has been evaluated extensively for basic decision support management and yield or water use predictions in China (He et al., 2013; Ji et al., 2014; Li et al., 2016; Zheng et al., 2016b). In this study, DSSAT Version 4.6 (Hoogenboom et al., 2011) was used to predict the number of days to maturity, water use, and productivity of winter wheat for the climate projections for 2020, 2040, 2060, 2080 and 2100 for rainfed conditions for locations at Baoji, Wugong and Weinan.

The minimum inputs for the CSM-CERES-Wheat model are daily weather data, soil profile characteristics, cultivar genetics, and crop management, such as planting date, plant population, row spacing, planting depth etc. at each location (Hunt and Boote, 1998; Hoogenboom et al., 2012). The weather inputs for the CERES-Wheat model include daily precipitation, maximum temperature (Tmax), minimum temperature (Tmin), and solar radiation. Long-term (1984–2013) daily records of rainfall, Tmax, Tmin and sunshine hours for the three locations were obtained from China Meteorological Data Service Center (CMDC) (http://data.cma.cn/) as reference years; daily solar radiation was determined based on a multivariate stochastic process using the observed daylight sunshine hours through WGEN (weather generator) in the DSSAT version 4.6 crop systems model (Garcia et al., 2008).

The weather inputs for simulating future projections were the reference weather data that modified based on SimCLIM. All of the four scenarios have different path shapes and emission targets, and both RCP 4.5 and RCP 6.0 belong to the middle-end scenario. In this study, we selected RCP 4.5 for its precedence over RCP 6.0 (Chen and Lin, 2011). Bao et al. (2015a) recommends that at least three GCMs should be selected in case the prediction is limited to a narrow representation of future climate. Therefore, the three GCMs selected for the present study were: the Beijing Climate Center, China Meteorological Administration's model BCC-CSM1 − 1 (BCC), the Queensland Climate Change Centre of Excellence and Commonwealth Scientific and Industrial Research Organization's model CSIRO-MK3-6-0 (CSIRO), and the NOAA Geophysical Fluid Dynamics Laboratory's model GFDL-CM3 (GFDL). Five resulting projections for weather data for 2020, 2040, 2060, 2080 and 2100 for Baoji, Wugong and Weinnan were generated with SimCLIM. Soil types and associated profile, surface and generic soil information were obtained from the China Soil Database (CSD). The soil types for the trial sites were silty clay loam for Baoji and Wugong and a clay loam for Weinan. More information about model calibration and evaluation can be found in Zheng et al. (2017) and Zheng et al. (2016b). The single cultivar "Xiaoyan22", the most common cultivar in the

Fig. 1. The location of three study sites in the Shaanxi Province (Guanzhong Plain).

Guanzhong Plain, was used for all three locations. The simulated number of days to maturity, grain yield and water use in the projections 2020, 2040, 2060, 2080 and 2100 were compared with the reference years (1984–2013).

3. Results

3.1. Climate projections

The climate change patterns including monthly solar radiation, precipitation, maximum temperature (Tmax) and minimum temperature (Tmin) for the projections for 2020, 2040, 2060, 2080 and 2100, were obtained using SimCLIM for Baoji, Wugong and Weinan. The changes were defined with respect to the baseline for the period 1961–1990 and the values varied by location, month and the respective GCMs that were used. Monthly solar radiation showed both a decrease and increase from the baseline depending upon which of the three GCMs was used. In general, the projections based on the CSIRO showed both the largest increase and decrease in solar radiation; there was a moderate change in solar radiation for the projections based on the GFDL, and the smallest change in solar radiation was for the projections based on the BCC. Similarly, the greatest change in monthly precipitation from the baseline was found for the projections based on the CSIRO, followed by the GFDL and BCC. Monthly Tmax and Tmin increased from 2020–2100 compared with the baseline for the projections for all three GCMs and the variation was similar.

For Baoji, the findings regarding changes in solar radiation, monthly precipitation, and Tmax and Tmin illustrated in Fig. 2. The change in monthly solar radiation from the baseline was small, and the change in different projections was the same based on the BCC. An extreme change occurred for September, October and November based on the CSIRO, which increased by 9.2%–21.7%, 11.1%–24.0% and then decreased by 14.6%–17.9%. The simulated change based on GFDL was intermediate between BCC and CSIRO. The smallest change in monthly precipitation from the baseline ranged from -0.9 % to 1.9 % for February for different projections based on the BCC, while the largest increase was ranged from 33.7%–46.9% for June. The largest increase in monthly precipitation ranged from 37.4%–76.2% for December for different projections based on the CSIRO, followed by June, which increased 34.9%–50.2% for different projections. For the GFDL, the prediction trend was similar with the BCC; however, the amplitude of variation in each month showed little difference. The simulated Tmax based on the three GCMs all increased compared with the baseline. Based on the BCC, the increase in temperature varied from 0.4 °C for August to 2.2 °C for February for 2020, and from 1.4 °C for August to 3.0 °C for February for 2100. While the increase in temperature varied from 0.7 °C for June to 3.0 °C for February for 2020, and from 2.1 °C for June to 5.3 °C for September for 2100 based on CSIRO. Based on GFDL, the increase in temperature varied from 0.8 °C for June and August to 2.6 °C for February for 2020 and from 1.4 °C for May to 4.1 °C for September for 2100.

For Wugong, the findings regarding changes in solar radiation, monthly precipitation, and Tmax and Tmin illustrated in Fig. 3. Generally, the changes from the baseline in monthly solar radiation for Wugong for the projections were larger than Baoji, and decreased compared to the baseline. An extreme change in solar radiation occurred in Januray, which decreased by 17.3%–14.9% compared to the baseline based on three GCMs. The change in precipitation for August and June showed the largest increase, among the different projections, ranging from 27.7 % for 2020 to 45.5 % for 2100 and 30.5 % for 2020 to 45.4 % for 2100 respectively. The Tmax increased from 2.5 °C for 2020 to 4.6 °C for 2100 for February and from 2.2 °C for 2020 to 4.0 °C for 2100 for September based on the CSIRO and GFDL respectively. The changes from baseline in monthly Tmin for Wugong were similar among the three GCMs.

For Weinan, the findings regarding changes in solar radiation, monthly precipitation, and Tmax and Tmin illustrated in Fig. 4. In general, the changes for Weinan for the projections for 2020–2100 were similar to those for Baoji, with a few exceptions. The projected solar radiation in June decreased based on three GCMs, and the increase was less than 20 %. Based on the GFDL, the largest change in solar radiation occurred from 1.8 % for 2020 to 2.4 % for 2100. The change in monthly precipitation decreased by 26.4 % in September for 2100 and followed by a decrease in May of 24.6 % for 2100 based on the BCC. The largest change in precipitation based on the CSIRO was in December, which was 35.7 % for 2020 and 90.1 % for 2100. While the largest change in precipitation based on the GFDL was for January, which was 23 % for 2020 and 51.3 % for 2100. The increase in temperature based on GFDL was the largest, followed by CSIRO and BCC. The increase in the monthly Tmax ranged from 0.5 °C to 1.5 °C for 2020 and and 0.9 °C–3.5 °C for 2100 based on BCC; from 0.6 °C to 1.9 °C for 2020 and 2.0 °C–4.4 °C for 2100 based on CSIRO; from 0.6 °C to 1.4 °C for 2020 and 1.1 °C–3.1 °C for 2100 based on GFDL.

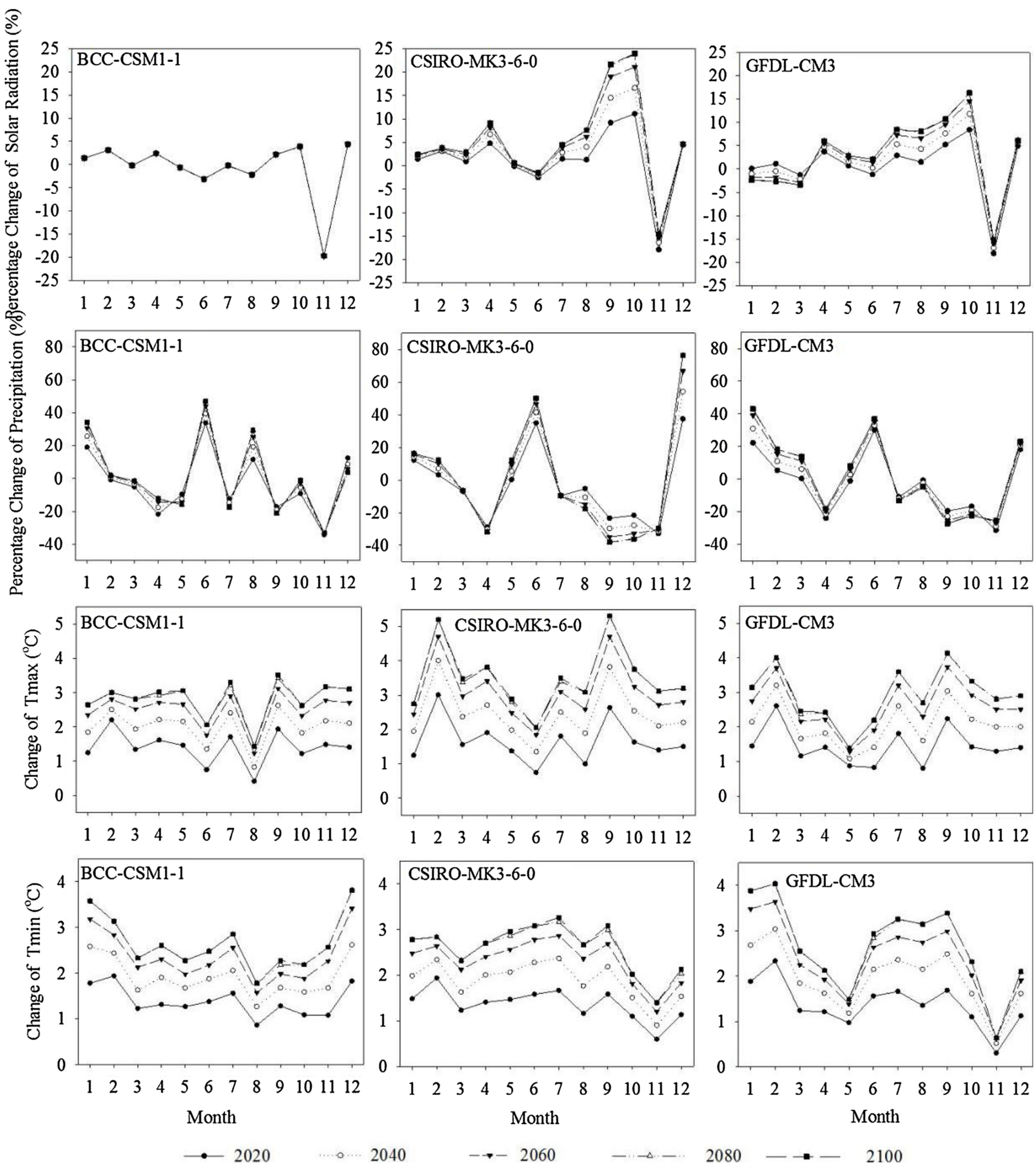

Fig. 2. Changes in monthly solar radiation (%), precipitation (%), maximum temperature (°C) and minimum temperature (°C) as projected for 2020, 2040, 2060, 2080 and 2100 based on RCP 4.5 for three GCMs compared to the baseline data for the period 1961-1990 for Baoji.

3.2. Wheat phenology projections

The number of days to maturity under rainfed conditions was simulated for the reference years and for the projections of 2020, 2040, 2060, 2080 and 2100. Each of the projections contained simulations for 30 years and the analysis is based on the average of 30 years. To determine the potential impact of climate change, the number of days to maturity was simulated for the 30 years of reference weather data for each location (Fig. 5). For Baoji, the number of days to maturity for the three GCMs was similar, ranging from 222 to 231, 222–232 and 225–232 days for the BCC, CSIRO and GFDL respectively. The change in number of days to maturity showed a decreasing trend based on all the GCMs, and the largest change was 13.2 days less than the reference years. The changes in number of days to maturity for Wugong and Weinan for the projections were similar to those for Baoji, which decreased compared to the reference years for all the GCMs. The largest change occurred in 2080 and 2100 with a decrease of 14.3 days based on CSIRO for Wugong, and occurred in 2080 with a decrease of 14.9 days based on CSIRO for Weinan. The number of days to maturity in all the areas decreased compared to the reference years, and it was clear that the increase in temperature was the major driver for the decrease in the number of days to maturity for the three locations. Because of the smaller increase in monthly mean temperature based on GFDL as compared to BCC and CSIRO, the number of days to maturity was also smaller based on GFDL in Baooji. While in Wugong and Weinan, the decrease in the number of days to maturity based on BCC was intermediate between CSIRO and GFDL, reflecting the fact that BCC also projected an intermediate increase in monthly temperature (Fig. 3).

3.3. Evapotranspiration projections

Average water demands for winter wheat was simulated for the 30

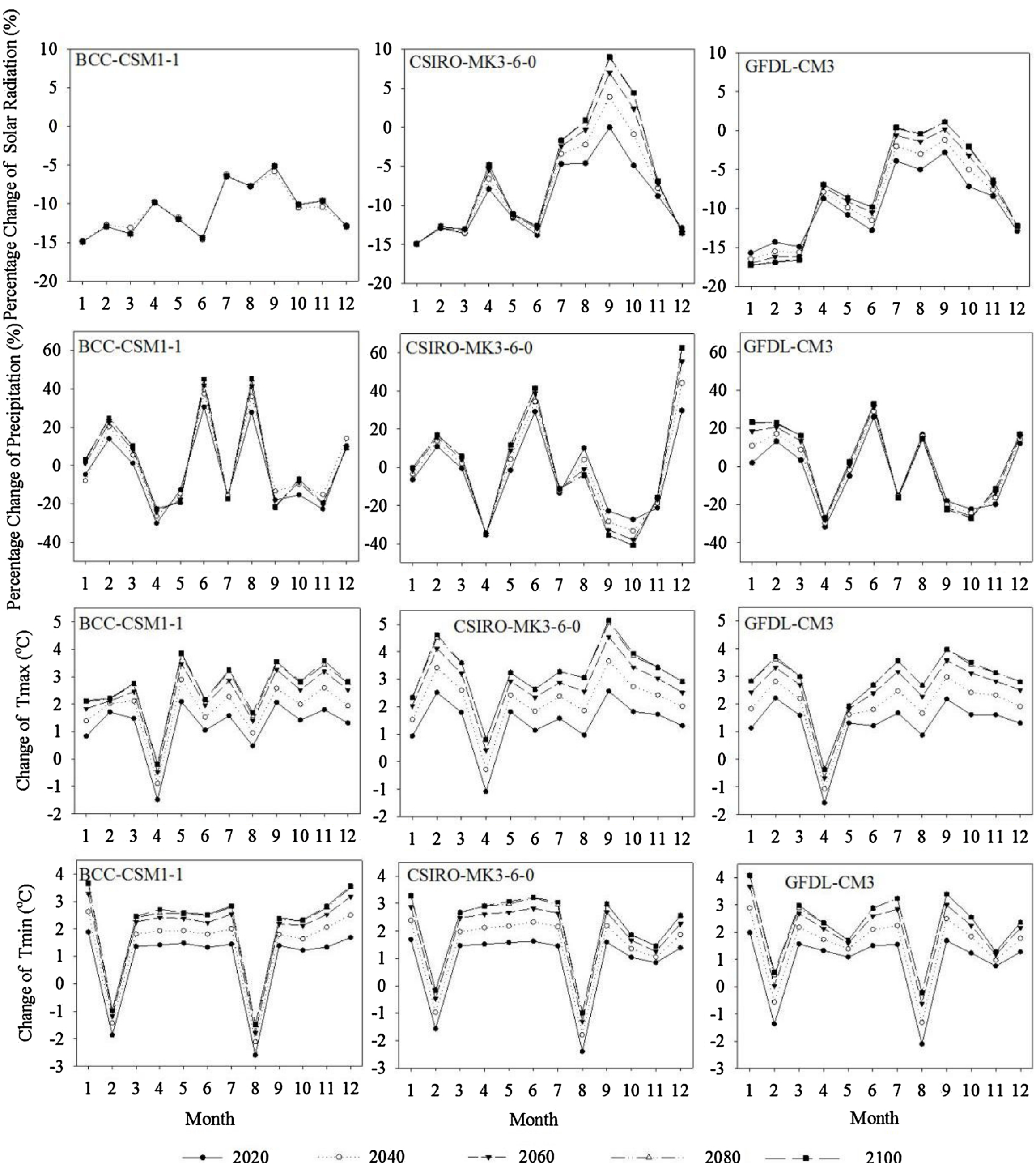

Fig. 3. Changes in monthly solar radiation (%), precipitation (%), maximum temperature (°C) and minimum temperature (°C) as projected for 2020, 2040, 2060, 2080 and 2100 based on RCP 4.5 for three GCMs compared to the baseline data for the period 1961-1990 for Wugong.

years of the reference data for Baoji, Wugong and Weinan, with evapotranspiration (ET) values of 312.0 mm, 280.5 mm and 356.3 mm, respectively. Simulated water demand for the winter wheat growth stage for the projections from 2020–2100 showed significant changes due to the effects of climate change (Fig. 6). For Baoji, the ET value changed from -11.6 mm–27.0 mm compared to the reference simulation, and for all the GCMs, the water demand of the growth stage decreased from 2020–2100. For the same period, ET for Wugong was similar to Baoji and the change varied from 11.7 mm to 35 mm for the different GCM projections. However, for the same period for Weinan, the increase in ET was greater for the projections based on the CSIRO and GFDL compared to the reference simulation. The simulated ET for Weinan was much larger than those two locations was due to the wheat grown in Weinan had a longer growing period.

3.4. Winter wheat yield projections

As discussed earlier, the historical weather data were modified with the climate change patterns using the outputs of the three GCMs coupled with RCP 4.5 scenario in three locations, and the projections were used for the prediction of winter wheat yield by using CERES-Wheat model. Rather than analyzing the absolute wheat yield predictions, our analysis was based on the differences between the wheat simulations for the reference years and those for 2020, 2040, 2060, 2080 and 2100 projections based on three GCM patterns (Fig. 7). In general, the number of days to maturity in the study area decreased compared to the reference years because of the increase in temperature, while yield increased due to the increase in precipitation and CO_2 concentration for the future projections.

For Baoji, the change in grain yield was -22.1%–3.5% based on the

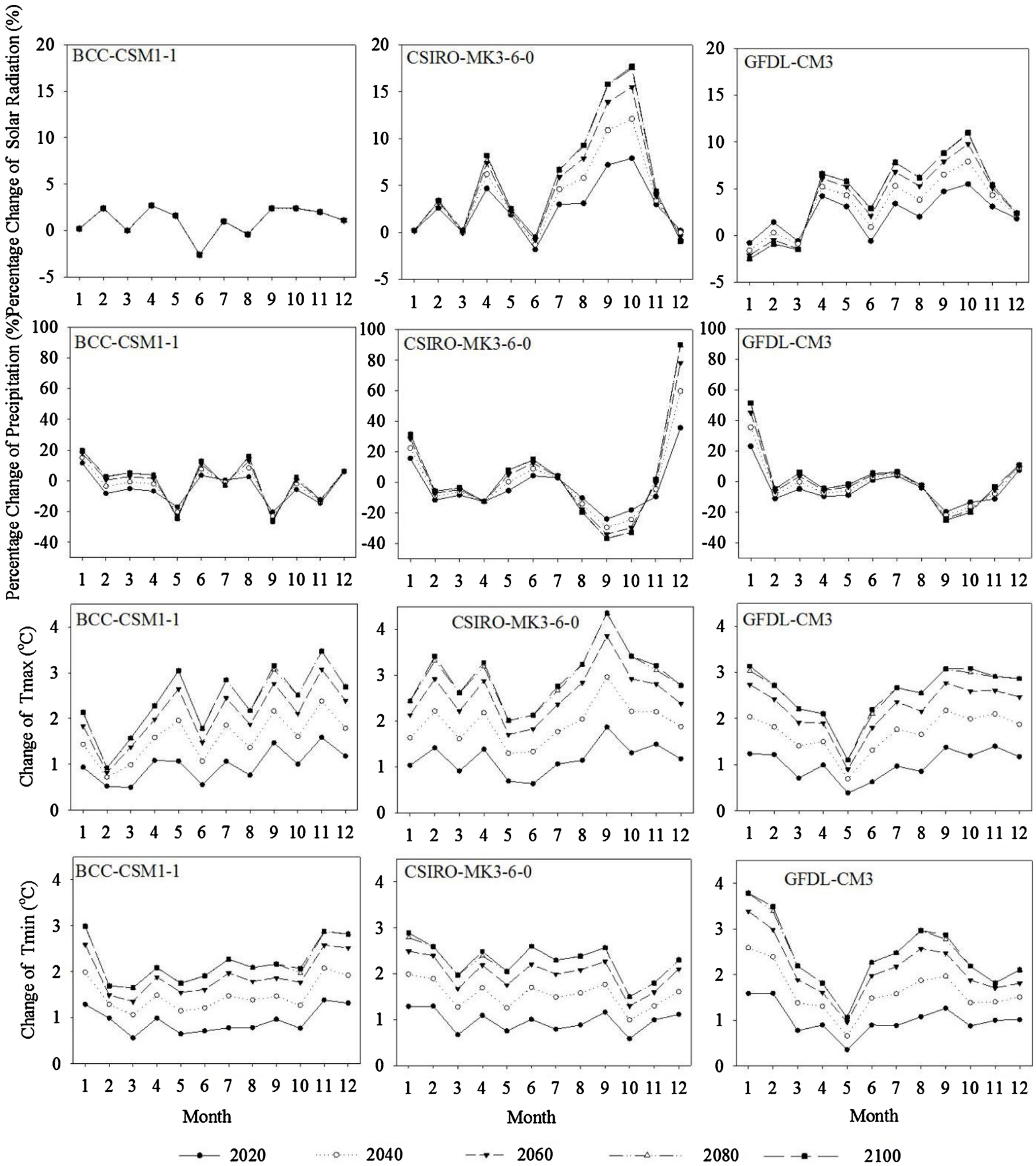

Fig. 4. Changes in monthly solar radiation (%), precipitation (%), maximum temperature (°C) and minimum temperature (°C) as projected for 2020, 2040, 2060, 2080 and 2100 based on RCP 4.5 for three GCMs compared to the baseline data for the period 1961-1990 for Weinan.

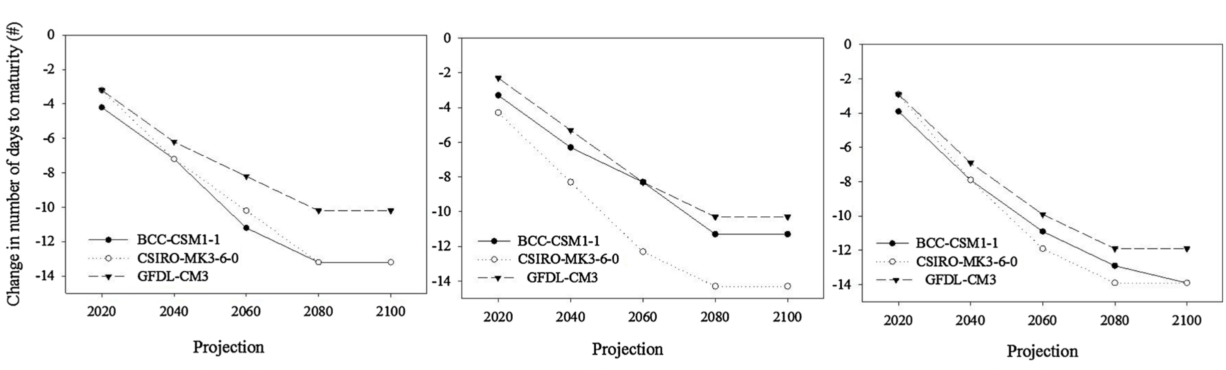

Fig. 5. Simulated number of days to maturity of winter wheat for three locations based on RCP 4.5 for three GCMs and different future projections.

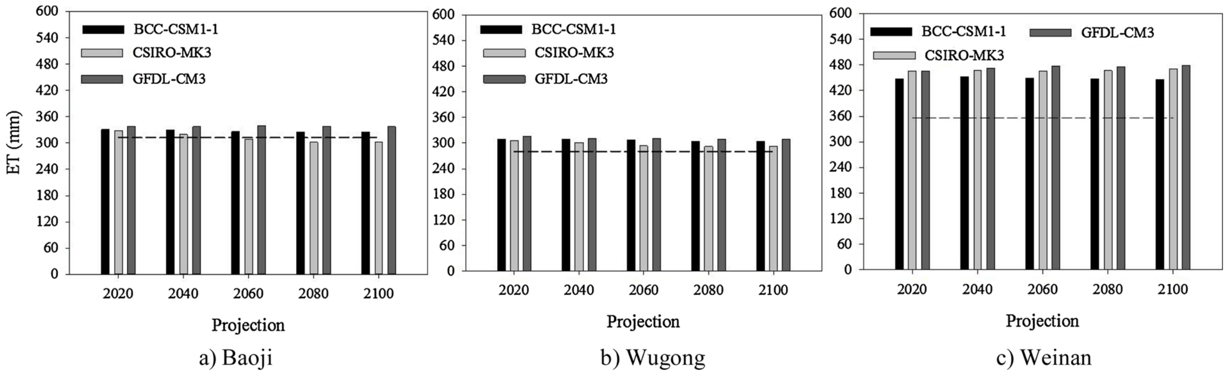

Fig. 6. Simulated evapotranspiration of winter wheat for three locations based on RCP 4.5 for three GCMs and different future projections.

CSIRO for 2060 and GFDL for 2020. The grain yield showed a decreasing trend from 2020 to 2060, and then it increased from 2060 to 2100. The decrease in yield with respect to the reference simulations was always larger for the CSIRO than for the other two GCMs, reflecting the fact that CSIRO also projected larger decrease in precipitation. Compared to Baoji, for Wugong, the increase in yield was 6.8%–21.7% based on the BCC and GFDL, while the change in yield ranged from -7.8 % to 0.4 % based on the CSIRO. Similarly, this was due to CSIRO generated the smallest increase in precipitation among the three GCMs, so the increase in rainfed yield was the lowest. However, the trend of change in yield for Weinan was little different from those for Baoji and Wugong. While the grain yield based on the three GCMs increased from 2020–2100 projections, the yield simulated by all the GCMs decreased before the 2060 projection compared with the reference year. The increases in yield for the 2060 and subsequent projections were larger than for the 2040 and 2020 projections because of the larger increase in precipitation and CO_2 concentration for the 2060 and the subsequent projections. The grain yield based on the CSIRO showed an increasing trend from the 2020 projection to the 2060 projection, with a slight decrease for the 2080 projection. The change in yield ranged from -7% to 7.5 %, -7.2%–10.8% and -4.9%–19% based on BCC, CSIRO and GFDL. Compared to BCC, the increase in rainfed yield based on GFDL was larger because of the larger increase in precipitation but showed a similar trend.

4. Discussion

In this study, the combination of different GCM outputs and the greenhouse gas emission scenario were used to assess the effects of climate change and its effect on winter wheat maturity dates, water use and grain yield across the Guanzhong Plain. The number of days to maturity decreased for all the locations. In general, there are many environmental factors that control crop phenology, such as temperature, photo period, water and nutrient status, etc. However, temperature is considered to be the main factor (McMaster and Wilhelm, 1997). Our simulations indicated a reduction of the period from sowing to maturity ranging from 2.3–14.9 days according to climate change projection and site (Fig. 5). The CSIRO predicted that the number of days to maturity for Baoji would be reduced from 235.2–222 days, from 233.3–219 days for Wugong and from 288.9–275 days for Weinan for the 2100 projection compared to the reference years, which was the largest decreasing among the three GCMs. This shortening effect was due to the warming climates rather than to the water shortage, since the primary effect of rainfall change and water availability on grain yield simulated by CERES-Wheat, and by the majority of crop growth models, is through limitations on growth, with no effect on crop development rate such as maturity date (Dettori et al., 2017). The results of our study are also consistent with those of Moriondo and Bindi (2007), who found a general reduction of the crop growing period of winter cereals (i.e. barley and wheat) in the entire Mediterranean Region in response to a 2 °C increase in temperature, with a decrease of the duration of the growing season ranging from 1.2 days in Tunisia to 12.2 days in Serbia.

The number of days to harvest maturity for the study area decreased for the different scenarios, thus also decreasing potential growth and yield due to a shorter growing season. The result are in agreement with the widely accepted evidence that shortening of the growth length is one of the main effects of climate change on crops, and it is one of the primary causes of projected decreases in yield (Parry et al., 2005). For the projection prior to 2060, the yield for Baoji showed a larger decrease compared to the yield for Wugong and Weinan. The yield based on the BCC and CSIRO models was less than the reference year for the projections, while the GFDL model showed larger than the reference year. This could be due to the variability in temperature for Baoji, especially in December and January, during the normally dormant phase of winter wheat. A significant increase in temperature could lead

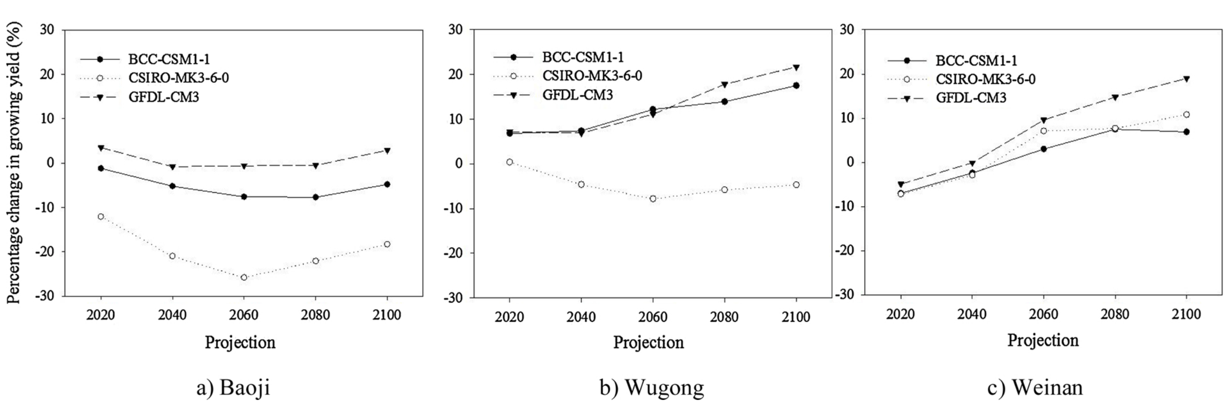

Fig. 7. Simulated grain yield of winter wheat for three locations based on RCP 4.5 for three GCMs and different future projections.

to rapid development of winter wheat during the early growth stage and an increase in tillering. This, in turn, could lead to the decline of heading rate and decrease yield. Yield normally decreases for wet and cool sites because of a reduction in vegetative development, LAI and thus potential intercepted radiation and consequently a lower biomass production over the course of the growing season (Wang et al., 2017). In our study, yield decreased when temperature was either too low or too high, with higher temperatures resulting in a significant reduction in yield. In addition, there was also an interaction among the temperature, rainfall and CO_2 concentration on wheat yields (Ludwig and Asseng, 2006). Different studies (Qu et al., 2019; Ventrella et al., 2012) explored the projected positive effect of slight temperature increase on wheat grain yield, possibly determined by the positive response of crops to elevated CO_2 concentration in the atmosphere, i.e. increase in photosynthesis rate or water-saving effect. The evidences from the experiments indicated that increase in CO_2 concentration could offset the negative effects (even enhance the positive effects) of future climate change on productivity of cereal crop caused due to the "CO_2-fertilization effect" (Parry et al., 2004). It was reported that the wheat yield would keep increasing until the CO_2 concentrate elevated to 890 ppm concluded by fitting both field and laboratory data (a least squares cubic equation) (Amthor, 2001). However, the present study did not take into account the physiological effect of projected high levels of CO_2, focusing the analysis on the impacts of changes in climate variables.

Precipitation is an important meteorological factor affecting winter wheat growth and yield. The seasonal distribution of precipitation in the Guanzhong Plain is uneven, and the water demand of winter wheat varies for the different growth phases. Precipitation early and late during the growing season only has small effect on the grain yield, while precipitation during the middle of the growing season, such as the jointing stage and flowering stage, has a significant positive effect on the final grain yield. This study of winter wheat in Northwest China showed that except for February, the monthly total precipitation during the winter months was positively correlated with wheat yield, while the precipitation during fallow period in June, July and August was negatively correlated with wheat yield (Zhang et al., 1996).

In this study, the response of winter wheat in the Guanzhong Plain to climate change under different scenarios showed differences due to the climate projections. The decrease in the number of days to maturity was mainly caused by an increase in temperature, similar to the findings of Alexandrov and Hoogenboom (2000). Yield for Baoji showed a decrease in yield, with the decrease in yield getting larger for projections later in the century. Yield for Wugong increased by 20 %, while, yield for Weinan increased gradually but showed the largest increase for all three sites of up to 41 %. Our results are slightly different from Yang et al. (2014) who showed that the grain yield for rainfed wheat increased for most of China compared with the reference year.

5. Conclusion

The present study found that future rainfall increased in February, June and December, and decreased in April, September and October for the Guanzhong Plain. Maximum and minimum temperature for most months increased compared to the baseline, with the largest increase in temperature for September and February. For all the three locations, the number of days to maturity decreased on average by 2–15 days based on three GCMs, while yield showed an increase after 2060 projection. Overall, this study found that the impact of climate change on winter wheat grown under rainfed conditions in the Guanzhong Plain was positive, while the impact differed among locations and some of the GCM projections. Some of the variability was due to the rainfed conditions that are more sensitive to climate change due to the uncertainty of future rainfall, temperature, solar radiation and other weather conditions. Future studies should include different wheat varieties that could be more heat tolerant and drought resistance and other potential adaptation scenarios.

Declaration of Competing Interest

The authors declare that there are no conflicts of interest.

Acknowledgements

This research was supported by the National Key Research and Development Program of China (2016YFC0400202, 2016YFC0400201), and the Project of Faculty of Agricultural Equipment of Jiangsu University. It was also part of the PhD project of Zhen Zheng, which was funded by the China Scholarship Council with the support of the AgWeatherNet Program at Washington State University, Prosser, Washington, USA. We wish to thank Xinchun Cao for his assistance in the preparation of this paper.

We greatly appreciate the careful and precise reviews by the anonymous reviewers and editors.

References

Abuodha, P.A.O., 2009. Application and Evaluation of Shoreline Segmentation Mapping Approaches to Assessing Response to Climate Change on the Illawarra Coast, South East Australia. (PhD Thesis). University of Wollongong, Australia. http://ro.uow.edu.au/theses/852/.

Alexandrov, V.A., Hoogenboom, G., 2000. Vulnerability and adaptation assessments of agricultural crops under climate change in the Southeastern USA. Theor. Appl. Climatol. 67, 45–63.

Amin, A., Nasim, W., Mubeen, M., Ahmad, A., Nadeem, M., Urich, P., Fahad, S., Ahmad, S., Wajid, A., Tabassum, F., Hammad, H.M., Sultana, S.R., Anwar, S., Baloch, S.K., Wahid, A., Wilkerson, C.J., Hoogenboom, G., 2018. Simulated CSM-CROPGRO-cotton yield under projected future climate by SimCLIM for southern Punjab, Pakistan. Agric. Syst. 167, 213–222.

Amthor, J.S., 2001. Effects of atmospheric CO_2 concentration on wheat yield: review of results from experiments using various approaches to control CO_2 concentration. Field Crops Res. 73, 1–34.

Asseng, S., Foster, I., Turner, N.C., 2011. The impact of temperature variability on wheat yields. Glob. Change Biol. 997–1012.

Asseng, S., Ewert, F., Martre, P., Rotter, R.P., Lobell, D.B., Cammarano, D., Kimball, B.A., Ottman, M.J., Wall, G.W., White, J.W., Reynolds, M.P., Alderman, P.D., Prasad, P.V.V., Aggarwal, P.K., Anothai, J., Basso, B., Biernath, C., Challinor, A.J., De Sanctis, G., Doltra, J., Fereres, E., Garcia-Vila, M., Gayler, S., Hoogenboom, G., Hunt, L.A., Izaurralde, R.C., Jabloun, M., Jones, C.D., Kersebaum, K.C., Koehler, A.K., Muller, C., Naresh Kumar, S., Nendel, C., O'Leary, G., Olesen, J.E., Palosuo, T., Priesack, E., Eyshi Rezaei, E., Ruane, A.C., Semenov, M.A., Shcherbak, I., Stockle, C., Stratonovitch, P., Streck, T., Supit, I., Tao, F., Thorburn, P.J., Waha, K., Wang, E., Wallach, D., Wolf, J., Zhao, Z., Zhu, Y., 2015. Rising temperatures reduce global wheat production. Nat. Clim. Change 5, 143–147.

Bao, Y., Hoogenboom, G., McClendon, R., Urich, P., 2015a. Soybean production in 2025 and 2050 in the southeastern USA based on the SimCLIM and the CSM-CROPGRO-Soybean models. Clim. Res. 63, 73–89.

Bao, Y., Hoogenboom, G., McClendon, R.W., Paz, J.O., 2015b. Potential adaptation strategies for rainfed soybean production in the south-eastern USA under climate change based on the CSM-CROPGRO-Soybean model. J. Agric. Sci. 153, 798–824.

Cammarano, D., Ceccarelli, S., Grando, S., Romagosa, I., Benbelkacem, A., Akar, T., Al-Yassin, A., Pecchioni, N., Francia, E., Ronga, D., 2019. The impact of climate change on barley yield in the Mediterranean basin. Eur. J. Agron. 106, 1–11.

Chen, M., Lin, E., 2011. Gloal greenhouse gas emission mitigation under representative concentration pathways scenarios and challenges to China. Adv. Clim. Change Res. 6, 436–442 (in Chinese with English abstract).

Chen, H., Li, L., Luo, X., Li, Y., Liu, D.L., Zhao, Y., Feng, H., Deng, J., 2019. Modeling impacts of mulching and climate change on crop production and N_2O emission in the Loess Plateau of China. Agric. For. Meteorol. 268, 86–97.

Darko, R., Yuan, S., Yan, H., Liu, J., Abbey, A., 2016. Calibration and validation of AquaCrop for deficit and full irrigation of tomato. Int. J. Agric. Biol. Eng. 9 (3), 104–110.

Dettori, M., Cesaraccio, C., Duce, P., 2017. Simulation of climate change impacts on production and phenology of durum wheat in Mediterranean environments using CERES-Wheat model. Field Crops Res. 206, 43–53.

Ding, D.Y., Feng, H., Zhao, Y., He, J.Q., Zou, Y.F., Jin, J.M., 2016. Modifying winter wheat sowing date as an adaptation to climate change on the loess plateau. Agron. J. 108, 53–63.

Ding, D., Zhao, Y., Feng, H., Hill, R.L., Chu, X., Zhang, T., He, J., 2018. Soil water utilization with plastic mulching for a winter wheat-summer maize rotation system on the Loess Plateau of China. Agric. Water Manage. 201, 246–257.

Flato, G., Marotzke, J., Abiodun, B., Braconnot, P., Chou, S.C., Collins, W., Cox, P., Driouech, F., Emori, S., Eyring, V., Forest, C., Gleckler, P., Guilyardi, E., Jakob, C., Kattsov, V., Reason, C., Rummukainen, M., Change, 2013. Evaluation of Climate Models. Climate Change 2013. The Physical Science Basis. Working Group I Contribution to the Fifth Assessment Report of the Intergovernmental Panel on Climate Change.

Garcia, A.Gy., Guerra, L.C., Hoogenboom, G., 2008. Impact of generated solar radiation

on simulated crop growth and yield. Ecol. Modell. 210, 312–326.
Gu, Z., Qi, Z., Ma, L., Gui, D., Xu, J., Fang, Q., Yuan, S., Feng, G., 2017. Development of an irrigation scheduling software based on model predicted crop water stress. Comput. Electron. Agric. 143, 208–221.
He, J., Cai, H., Bai, J., 2013. Irrigation scheduling based on CERES-Wheat model for spring wheat production in the Minqin Oasis in Northwest China. Agric. Water Manage. 128, 19–31.
He, L., Asseng, S., Zhao, G., Wu, D., Yang, X., Zhuang, W., Jin, N., Yu, Q., 2015. Impacts of recent climate warming, cultivar changes, and crop management on winter wheat phenology across the Loess Plateu of China. Agric. For. Meteorol. 200, 135–143.
Hoogenboom, G., Jones, J.W., Winkens, P.W., Porter, C.H., Boote, K.J., Hunt, L.A., et al., 2011. Decision Support System for Agrotechnology Transfer, Version 4.5. Univ. of Hawaii, Honolulu.
Hoogenboom, G., Jones, J.W., Traore, P.C.S., Boote, K.J., 2012. Experiments and data for model evaluation and application. In: Kihara, J., Fatondji, D., Jones, J.W., Hoogenboom, G., Tabo, R., Bationo, A. (Eds.), Improving Soil Fertility Recommendations in Africa Using the Decision Support Systems for Agrotechnology Transfers (DSSAT). Springer, Dordrecht, the Netherlands, pp. 9–18.
Hoogenboom, G., Porter, C.H., Boote, K.J., Shelia, V., Wilkens, P.W., Singh, U., White, J.W., Asseng, S., Lizaso, J.I., Moreno, L.P., Pavan, W., Ogoshi, R., Hunt, L.A., Tsuji, G.Y., Jones, J.W., 2019. The DSSAT crop modeling ecosystem. In: Boote, K.J. (Ed.), Advances in Crop Modeling for a Sustainable Agriculture. Burleigh Dodds Science Publishing, Cambridge, United Kingdom, pp. 173–216.
Hunt, L.A., Boote, K.J., 1998. Data for model operation, calibration, and evaluation. In: Tsuji, G.Y., Hoogenboom, G., Thornton, P.K. (Eds.), Understanding Options for Agricultural Production. Kluwer Academic Publishers, Dordrecht, pp. 9–39.
IPCC, 2007. Climate change 2007: impacts, adaptation and bulnerability. In: Parry, M.L., Canziani, O.F., Palutikof, J.P., van der Linden, P.J., Hanson, C.E. (Eds.), Contribution of Working Group IIto the Fourth Assessment Report of the Inter Governmental Panel on Climate Change. Cambridge University Press, UK, Cambridge, pp. 589–662.
IPCC, 2014. Climate change 2014: synthesis report. In: Pachauri, R.K., Meyer, L.A. (Eds.), Contribution of Working Groups I, II and III to the Fifth Assessment Report to the Intergovernmental Panel o Climate Change [Core Writing Team. IPCC, Geneva, Swizerland, pp. 151 In IPCC AR5 Synthesis Report website.
Ji, J., Cai, H., He, J., Wang, H., 2014. Performance evaluation of CERES-Wheat model in Guanzhong Plain of Northwest China. Agric. Water Manage. 144, 1–10.
Jones, J.W., Hoogenboom, G., Porter, C.H., Boote, K.J., Batchelor, W.D., Hunt, L.A., Wilkens, P.W., Singh, U., Gijsman, A.J., Ritchie, J.T., 2003. The DSSAT cropping system model. Eur. J. Agron. 18, 235–265.
Karimi, T., Stöckle, C.O., Higgins, S., Nelson, R., 2018. Climate change and dryland wheat systems in the US Pacific Northwest. Agric. Syst. 159, 144–156.
Kristensten, K., Schelde, K., Olesen, J.E., 2011. Winter wheat yield response to climate variability in Denmark. J. Agric. Sci. 149, 33–47.
Li, Z., Song, M., Feng, H., Zhao, Y., 2016. Within-season yield prediction with different nitrogen inputs under rain-fed condition using CERES-Wheat model in the northwest of China. J. Sci. Food Agric. 96, 2906–2916.
Liang, S., Li, Y., Zhang, X., Sun, Z., Sun, N., Duan, Y., Xu, M., Wu, L., 2018. Response of crop yield and nitrogen use efficiency for wheat-maize cropping system to future climate change in northern China. Agric. For. Meteorol. 262, 310–321.
Liu, C., Qi, Z., Gu, Z., et al., 2017a. Optimizing irrigation rates for cotton production in an extremely arid area using RZWQM2-Simulated water stress. Trans. ASABE 60 (6), 2041–2052.
Liu, J., Du, H., Wu, Z., He, H.S., Wang, L., Zong, S., 2017b. Recent and future changes in the combination of annual temperature and precipitation throughout China. Int. J. Climatol. 37, 821–833.
Ludwig, F., Asseng, S., 2006. Climate change impacts on wheat production in a Mediterranean environment in Western Australia. Agric. Syst. 90 (1), 159–179.
McMaster, G., Wilhelm, W., 1997. Growing degree-days: one equation, two interpretations. Agric. For. Meteorol. 87, 291–300.
Mo, F., Sun, M., Liu, X.-Y., Wang, J.-Y., Zhang, X.-C., Ma, B.L., Xiong, Y.-C., 2016. Phenological responses of spring wheat and maize to changes in crop management and rising temperatures from 1992 to 2013 across the Loess Plateau. Field Crops Res. 196, 337–347.
Moriondo, M., Bindi, M., 2007. The impact of climate change on the phenology of typical Mediterranean crops. Ital. J. Agrometeorol. 3, 5–12.
Olesen, J.E., Trnka, M., Kersebaum, K.C., Skjelvag, A., Seguin, B., Peltonen-Sainio, P., Rossi, F., Kozyra, J., Micale, F., 2011. Impacts and adaptation of European crop production systems to climate change. Eur. J. Agron. 34, 96–112.
Parry, M., Rosenzweig, C., Iglesias, A., Livermore, M., Fischer, G., 2004. Effects of climate change on global food production under SRES emissions and socio-economic scenarios. Global Environ. Change 14, 53–67.
Parry, M., Rosenzweig, C., Livermore, M., 2005. Climate change, global food supply and risk of hunger. Philos. Trans. R. Soc. Lond. Ser. B 360 (1463), 2125–2138.
Peng, S.B., Huang, J.L., Sheehy, J.E., Laza, R.C., Visperas, R.M., Zhong, X., Centeno, G.S., Khush, G.S., Cassman, K.G., 2004. Rice yield decline with higher night temperature from global warming. Proc. Natl. Acad. Sci. U. S. A. 101, 9971–9975.
Qu, C., Li, X., Ju, H., Liu, Q., 2019. The impacts of climate change on wheat yield in the Huang-Huai-Hai Plain of China using DSSAT-CERES-Wheat model under different climate scenarios. J. Integr. Agric. 18 (6), 1379–1391.
Sommer, R., Glazirina, M., Yuldashev, T., Otarov, A., Ibraeva, M., Martynova, L., Bekenov, M., Kholov, B., Ibragimov, N., Kobilov, R., Karaev, S., Sultonov, M., Khasanova, F., Esanbekov, M., Mavlyanov, D., Isaev, S., Abdurahimov, S., Ikramov, R., Shezdyukova, L., de Pauw, E., 2013. Impact of climate change on wheat productivity in Central Asia. Agric. Ecosyst. Environ. 178, 78–99.
Storey, L.P., 2009. Effect of Climate and Land Use Change on Invasive Species: A Case Study of Tradescantiafluminensis(Vell.) in New Zealand. PhD Dissertation University of Waikato, Hamilton. http://hdl.handle.net/10289/2634.
Tao, F., Yokozawa, M., Xu, Y., Hayashi, Y., Zhang, Z., 2006. Climate changes and trends in phenology and yields of field crops in China, 1981–2000. Agric. For. Meteorol. 138, 82–92.
Tao, F., Yousay, H., Zhang, Z., Toshihiro, S., Yokozawa, M., 2008. Global Warming, Rice Production, and Water Use in China.
Tao, F., Zhang, Z., 2013. Climate change, wheat productivity and water use in the North China Plain: a new super-ensemble-based probabilistic projection. Agric. For. Meteorol. 170, 146–165.
Ventrella, D., Charfeddine, M., Moriondo, M., Bindi, M., 2012. Agronomic adaptation strategies under climate change for winter durum wheat and tomato in southern Italy: irrigation and nitrogen fertilization. Reg. Environ. Change 12, 407–419.
Wang, Q.X., Fan, X.H., Z.D, Q, Wang, M.B, 2012. Change trends of temperature and precipitation in the Loess Plateau Region of China, 1961-2010. Glob. Planet. Change 92-93, 138–147.
Wang, B., Liu, D., Asseng, S., Macadam, I., Yu, Q., 2017. Modelling wheat yield change under CO_2 increase, heat and water stress in relation to plant available water capacity in eastern Australia. Eur. J. Agron. 90, 152–161.
Warrick, R.A., 2007. SimCLIM: Recent Developments of an Integrated Model for Multiscale, Risk-based Assessments of Climate Change Impacts and Adaptation. in: the 2007 ANZSEE Conference Papers. Australia-new Zealand Society for Ecological Economics. www.anzsee.org./2007 conference/conference_papers.asp (Accessed on 21 Jan 2015). .
Warrick, R.A., 2009. Using SimCLIM for modelling the impacts of climate extremes in a changing climate: a preliminary case study of household water harvesting in Southeast Queensland. Modsim Congress 2583–2589.
Yan, C.R., Liu, L., Huang, G.H., 2018. Multi-model projections of future climate change under different RCP scenarios in arid inland region of north China. J. Drain. Irrig. Mach. Eng. 36, 1193–1199 (in Chinese with English abstract).
Yang, W.C., Mao, X.M., 2018. Uncertainty of crop models under influence of climate change. J. Drain. Irrig. Mach. Eng. 36, 874–879 902. (in Chinese with English abstract).
Yang, X., Tang, X., Chen, B.D., Tian, Z., Zhao, S.J., 2014. Impacts of climate change on wheat yield in china simulated by CMIP5 Multi-Model Ensembel projecitions. Sci. Agric. Sin. 47, 3009–3024 (in Chinese with English abstract).
Yin, C., Li, Y., Urich, P., 2013. SimCLIM 2013 Data Manual. CLIMsystems Ltd.
Zhang, Z.B., Shan, L., Wang, D.X., 1996. Optimum regression model between rainfall and wheat yield. Bull. Soil Water Conserv. 16, 31–34 50. (in Chinese with English abstract).
Zheng, Z., Cai, H., Hoogenboom, G., Chaves, B., Yu, L., 2016a. Limited irrigation for improving water use efficiency of winter wheat in the Guanzhong Plain of Northwest China. Trans. ASABE 59, 1841–1852.
Zheng, Z., Cai, H.J., Yu, L.Y., Wang, J., 2016b. Comparison of two crop evapotranspiration calculating approaches in CSM-CERES-Wheat model. Trans. Chin. Soc. Agric. Mach. 47, 179–191 (in Chinese with English abstract).
Zheng, Z., Cai, H., Yu, L., Hoogenboom, G., 2017. Application of the CSM–CERES–Wheat model for yield prediction and planting date evaluation at Guanzhong Plain in Northwest China. Agron. J. 109, 204.